Received: 22 October 2021 | Revised: 7 June 2022 | Accepted: 24 August 2022

DOI: 10.1002/cpe.7348

RESEARCH ARTICLE

WILEY

Breast lesion identification and categorization using mammography screening based on combined convolutional recursive neural network framework with parameters optimized using multi-objective seagull optimization algorithm

N. K. Sakthivel[1] | **S. Subasree**[2] | **Pachhaiammal Alias Priya M**[3] | **Amit Kumar Tyagi**[4]

[1]Dean, Nehru Institute of Engineering and Technology, Tamil Nadu, India

[2]Professor and Head, Department of Computer Science and Engineering, Nehru Institute of Engineering and Technology, Coimbatore, Tamil Nadu, India

[3]Department of Artificial Intelligence and Data Science, Sri Sairam Institute of Technology, Chennai, Tamil Nadu, India

[4]School of Computer Science and Engineering, Vellore Institute of Technology, Chennai, Tamil Nadu, India

Correspondence
N. K. Sakthivel, Nehru Institute of Engineering and Technology, Coimbatore, Tamil Nadu, India.
Email: drnksakthivelphd@gmail.com

Summary

In recent years, a number of learning methods have been adopted for classifying the mammogram images, which helps the early detection and diagnosis of breast cancer. The breast lesion identification and categorization using mammography screening based on combined convolutional neural network and recursive neural network (CRNN) framework with parameters optimized using multi-objective seagull optimization algorithm (BLIC-CRNN-MOSOA) is proposed in this article. Initially, the unnecessary noise components are taken away from the mammogram images and the quality of the images are enhanced based on altered phase preserving dynamic range compression filtering approach. Then, the deep CRNN model with weight parameters optimized using multi-objective seagull optimization algorithm is adopted for classifying the mammogram images into three categories: (i) normal, (ii) benign, and (iii) malignant masses. The proposed BLIC-CRNN-MOSOA approach is executed in MATLAB platform, and its performance is compared with other deep learning classification approaches. Then the simulation performance of the proposed BLIC-CRNN-MOSOA method attains higher accuracy 99.67%, 98.38%, and 97.45%, higher sensitivity 98.33%, 89.34%, and 88.96%, higher specificity 93.15%, 91.25%, and 92.88% compared with existing methods, like BLIC-FrCN, BLIC-ICS-ELM, and BLIC-DCNN-BO. By this, the proposed method achieves higher classification accuracy with less misclassified error. Finally, the simulation results show that the proposed method is more efficient than the other classification methods.

KEYWORDS

altered phase preserving dynamic range compression, breast cancer, convolutional neural networks, multi-objective seagull optimization algorithm, recursive neural networks

1 | INTRODUCTION

Breast cancer is one type of cancer that forms in the cells of the breasts. Women are mostly affected by this disease. In United States, new cases are reported as 0.25 million and mortality as 0.04 million.[1] Around one in eight women affected this disease in developed countries. A report states that the breast cancer is considerably raised globally.[2] A routine imaging procedure for screening is mammography.[3] It creates higher

quality imageries to display the internal structure of breast as well as measure the breast density. It plays a significant role of early detection.[4] Massive computer-aided diagnosis (CAD) systems are studied for certain purposes, like malignant/benign categorization, subtype disease diagnosis.[5–7] Typical methods focused on selecting proficient and discriminating features and integrating the system with parameters tuned through supervised learning, namely, artificial neural network (ANN), support vector machine (SVM).[8,9] General utilized features through intensity statistics, shape descriptors, texture descriptors, invariant moments, and multiple scale feature descriptors.[10,11] Recently, the deep learning has modernized the object recognition as well as image representation fields.[12] Unlike typical methods, deep learning delineates the convolutional neural network (CNN) structure that adapts to simulate human-like information abstraction and retrieves lower medium and higher level features directly from raw imagery patches.[13,14]

The complex context of the classification procedure in classical deep learning models lessens the efficiency and accuracy of the system. The existing methods did not give adequate exactness, also error rate was raised. When screening the mammogram imageries, these methods are employed to illustrate the misclassification errors. But the proposed approach is feasible in real time applications to screen the abnormalities at beginning stage, thus, scaling the most appropriate treatment to the patient to minimize death. The major intention of this work is "to detect the breast cancer at initial stage with higher accuracy by decreasing the computational time with error rate."

The major contributions of this article are:

- An efficient detection and classification model using MOSOA for the detection of beginning stage breast cancer.
- At first, the image preprocessing with feature extraction is carried out to preserve the helpful information, and then extract the desired features.
- The phase preserving dynamic range compression (APPDRC) filtering technique preserves the local features in the image, thereby compressing the images dynamic range for better boundary detection.
- A combined deep learning based classification model using CNN with RNN is employed to classify the mammogram images as three categories: benign, the malignant, and the normal with improved classification accuracy.
- A combined deep learning based on CRNN framework possesses the ability to concern the image content and learn the images structured feature.
- The weight parameters for deep learning framework are initialized and adjusted with the help of MOSOA.
- The proposed approach is activated in MATLAB, its performance is analyzed under performance metrics.
- The mammogram imageries are taken through MAMMOSET dataset, a compilation of datasets consisting of regions of interest (ROIs) of different mammogram images.

The remainder of this article is organized as: Section 2 portrays the recent studies, Section 3 explains about the proposed methodology, Section 4 demonstrates the experimental outcomes, Section 5 concludes the article.

2 | RELATED WORKS

Among various research works on breast lesion identification and categorization using mammogram images, a certain recent works are described here.

Al-Antari et al.[15] have suggested a deep learning CAD for breast lesion in digital mammogram. A deep learning base integrated computer-aided diagnosis was deemed to detect breast lesions from digital x-ray mammograms including identification, separation, and categorization. A full resolution convolutional network as well as separation model of deep network was employed to segment the breast lesions. Finally, three conventional deep learning approaches involving regular feed forward CNN, ResNet-50, Inception ResNet-V2 were applied to categorize as benign or malignant. It provides high sensitivity conversely with high error rate.

Chakravarthy and Rajaguru[16] have presented an automatic identification and categorization of mammograms utilizing enhanced extreme learning machine along deep learning. The digital mammograms were taken from CBIS-DDSM, Mammographic Image Analysis Society and IN breast datasets. In which, 570 digital mammograms from CBIS-DDSM dataset, 322 digital mammograms from Mammographic Image Analysis Society and 179 full-field digital mammograms from IN breast dataset for assessment. ResNet-18 base deep extracted features with presented improved crow-search optimized extreme learning machine approach were utilized. It provides minimum classification accuracy with lower error rate.

Hizukuri et al.[17] have presented CAD system for differentiating benign and malignant masses on breast DCE-MRI imageries utilizing DCNN and Bayesian optimization. The CAD differentiate the benign and malignant breast masses by DCNN with Bayesian optimization. Where, initially determined a baseline DCNN model from familiar DCNN depending on classification presentation. The structure of DCNN was determined by changing the hyper parameters of the baseline DCNN model, namely, count of layers, filter size, count of filters using Bayesian optimization. It provides lower classification accuracy with minimum sensitivity.

Al-Antari et al.[18] have presented the assessment of deep learning identification and categorization toward CAD of breast lesions in digital x-ray mammograms. An incorporated computer-aided diagnosis of deep learning identification and categorization was presented to enhance the diagnostic presentation of breast lesions. The regular feed forward CNN, ResNet-50, InceptionResNet-V2 were the three deep learning classifiers, which modified for breast lesion categorization. The presented method was assessed over 5-fold cross-validation tests with digital x-ray mammograms DDSM and IN breast. It provides lower detection accuracy and higher misclassified error.

Melekoodappattu and Subbian[19] have presented automated breast cancer detection using hybrid extreme learning machine classifier. The classification approaches predict the class label for unlabeled dataset depending on its proximity of learnt pattern. The selected features derived after feature selection was categorized into three classes by extreme learning machines: normal, benign, and malignant. Lower generalization performance occurs owing to ill-conditioned output matrix of the hidden layer of the classifier. It attains better sensitivity with lower classification accuracy.

Cao et al.[20] have presented a study of breast lesion identification and categorization from ultrasound imageries utilizing deep learning models. Where, the presentation of other classification methods was evaluated for breast lesions CAD. To attain that, dataset contains 579 benign and 464 malignant lesion cases with related ultrasound imageries manually annotated by experienced clinicians. It provides higher precision and F-Measure conversely with high misclassified error.

3 | PROPOSED METHODOLOGY

In this work, a deep learning model that combines the features of CNN with RNN is employed to the breast masses classification as various classes. For the combined (CNN-RNN) network, the weight parameters are optimized using MOSOA. The mammogram imageries are taken from MAMMOSET dataset for classification. This database consists of different mammogram imageries, like benign, malignant, and normal.

3.1 | Overall structure of the proposed classification model

Figure 1 depicts the proposed CRNN-MOSOA based on breast cancer classification framework.

3.1.1 | Preprocessing

This is the primary step in all types of the applications of image processing. The raw image has certain unnecessary noise along artifacts. The preprocessing step eliminates the unnecessary noise from the image with the help of filtering approaches. Therefore, the noise-free clean image is more required. In the proposed work, an APPDRC[21] based filtering technique is utilized to preserve the local features. This filtering approach also eliminates the noise components from the image.

Preprocessing depending on APPDRC approach

To preserve the local features, APPDRC based filter is used, by this, the dynamic range of an image is compressed. The local phase is extracted by the APPDRC filtering approach and amplitude of an image using different monogenic filters. Here, a range of reducing function is applied to the amplitude values for reducing the dynamic range of image. The reconstructed image has only phase values. Therefore, the output image maintains feature reliability within the minimized dynamic range. APPDRC filtering method has two major properties: the local phase data is secured, and the scale of analysis is regulated by selecting appropriate spatial frequencies during image reconstruction phase. This is carried out by certain high-pass filters.

Here, the local phase with amplitude is acquired through the monogenic filters. The monogenic filters are formed by combining high pass filter or radial band-pass filter along Riesz transform. This is 2D transform same as that of Hilbert transform. These are covered by several filters on two-dimensional frequency domain (x_1, x_2). This is expressed in Equation (1):

$$H_1 = i\frac{x_1}{\sqrt{x_1^2 + x_2^2}}, \quad H_2 = i\frac{x_2}{\sqrt{x_1^2 + x_2^2}}, \tag{1}$$

where the vector $H = (H_1, H_2)$ denotes the spatial representation of convolutional kernel of Riesz transform, x denotes coordination of pixels.

The local phase including image amplitude I is derived by convolving the imagery with high-pass or band-pass filters f along 2 Riesz transformed filtered versions $h_1 f$ and $h_2 f$ of high-pass filters or band-pass filters.

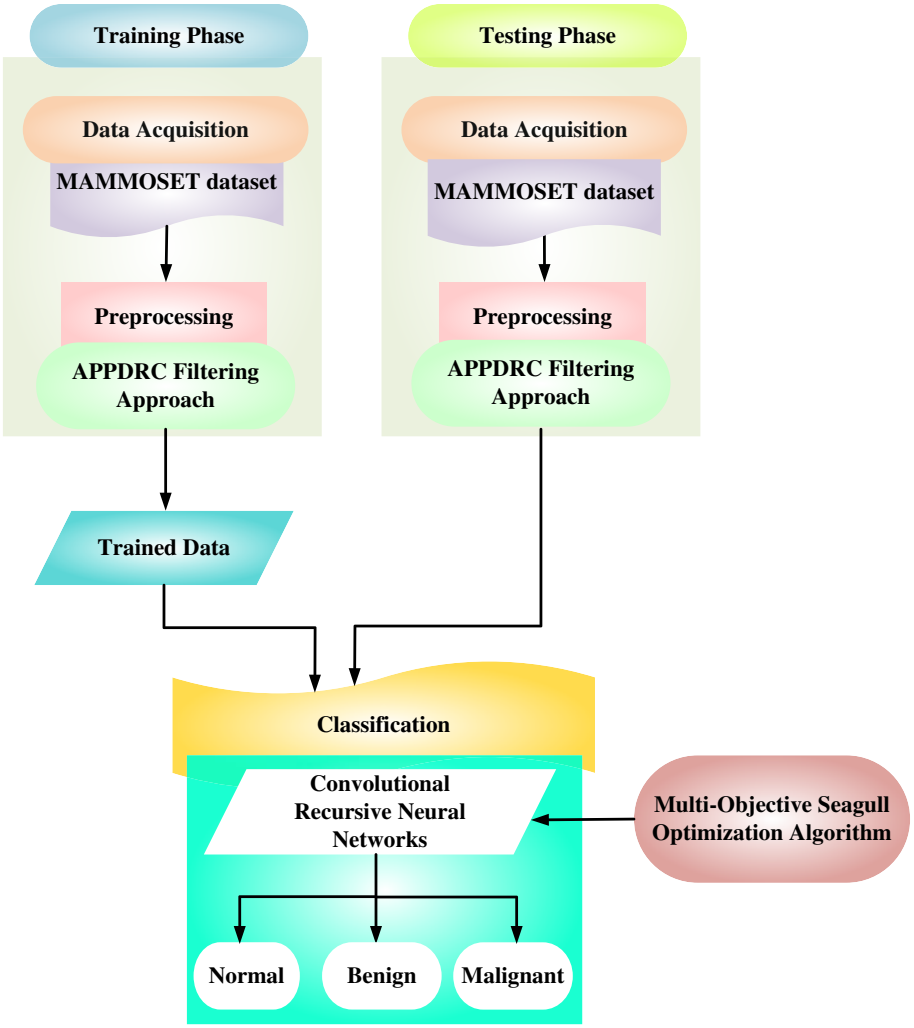

FIGURE 1 Overall structure of proposed BLIC-CRNN-MOSOA method

The local amplitude in the location of image (u, v) is expressed as

$$A(u,v) = \sqrt{f(u,v)^2 + h_1 f(u,v)^2 + h_2 f(u,v)^2}. \tag{2}$$

In image location (u, v), the local phase is exhibited as

$$\phi(u,v) = a\tan 2\left(f(u,v)\right), \sqrt{h_1 f(u,v)^2 + h_2 f(u,v)^2}. \tag{3}$$

Also, the orientation is exhibited as

$$\theta(u,v) = a\tan 2\left(h_2 f(u,v), h_1 f(u,v)\right). \tag{4}$$

The reconstructed image along tone-mapped values is

$$T(u,v) = \log(A(u,v) + 1) \cdot \sin(\phi(u,v)). \tag{5}$$

The fine information is preserved from the image depending on high pass filters. The high pass filters possess the capability to retain the high-frequency signal components.

Thus, from the image, the unnecessary noise components are eliminated for better boundary or edge detection.

3.1.2 | Feature extraction

While the context of feature extraction, the important features are extracted from the image. In which extracted several modes of textural including shape features. The process of feature extraction averts the data over fitting while classification, it helps to attain feasible classification outcomes. A few important features, namely, area, radius, perimeter smoothness used for processing the breast mammogram imageries at the classification state.

3.1.3 | Classification

In this article, the mammogram imageries are classified as three types: normal, benign, malignant masses using combined deep learning framework (CRNN) utilizes MOSOA for optimizing the loss functions.

Architecture of combined CRNN framework

The deep learning method benefits from high amount of data for training. Therefore, deep learning based image classification is well suitable for classifying large number of mammogram images. The typical architecture of CRNN framework is depicted in Figure 2:

The combination of CNN and RNN is termed as CRNN. This combined model is used as a classifier to classify the mammogram images into different categories. The proposed CRNN model integrates the features of CNNs and RNNs to obtain the better classification of mammogram images. The proposed CRNN model is built by an input layer, a hidden layer, and an output layer and also the proposed model is built by pretrained CNN layer, a RNN layer, a merge layer, fully-connected, softmax output.

CRNN[22] model, the low-level invariant features are learned by the convolutional neural network layer. These invariant features are fed as input to RNNs creates the features with higher order. The output from the CNN is transferred to long short term memory (LSTM) located in the RNN. Thus, the whole CNN-RNN model is trained for classification of mammogram images.

The proposed classification framework consists of both training and testing phases: The convolution NN is pretrained using images obtained from the MAMMOSET database during the training phase. Then, the transmission learning scheme is used to initialize the CNN model with pretrained network parameters. After that, all the convolutional NN layers are kept stable for training the recursive neural network layer.

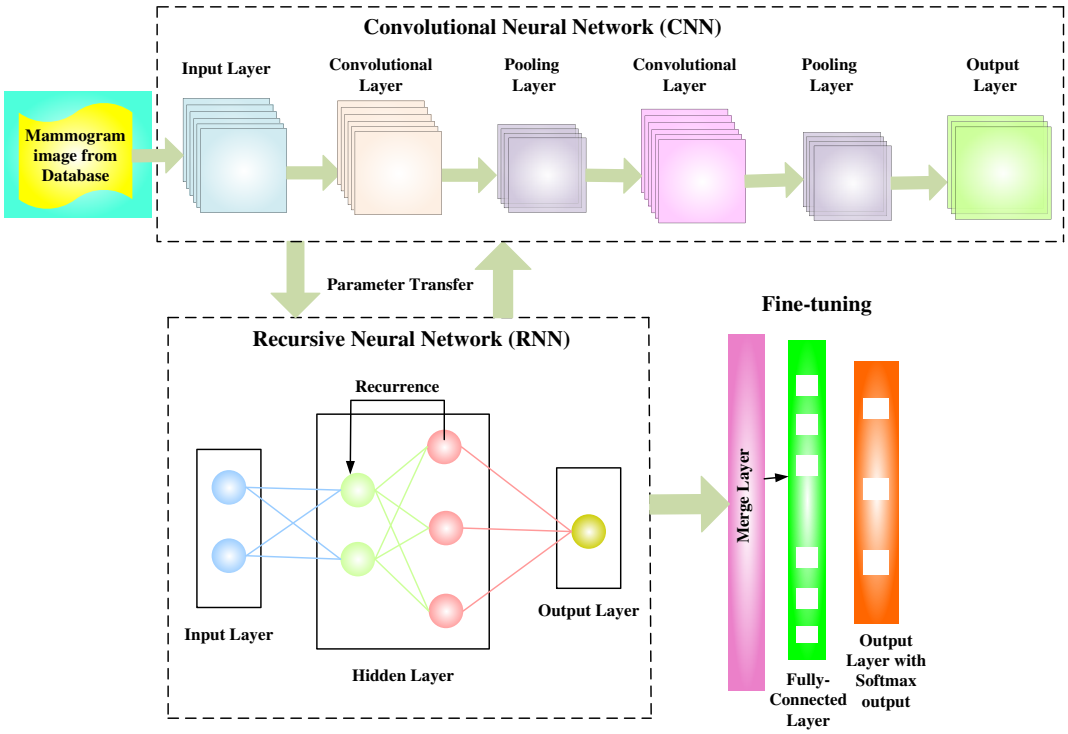

FIGURE 2 Typical architecture of CRNN model

Then, the features of both convolutional NN wither cursive NN are merged with the help of neural network attention schemes. At the testing phase, the pretrained imagery is fed as input to the fine-tuned CRNN mode. Finally, the classification outcomes acquire at the softmax layer.The layers in the overall CRNN classification model are explained as follows:

Pretrained CNN layer:

The pretrained weight parameters are used for initializing the weight functions in CNN mode. The CNN mode is constituted by a combination of convolutional layers and pooling layers.

Convolutional layer:

Here, several convolutional windows with various sizes are employed to perform convolution with feature maps from the previous layer. The convolutional windows are placed sequentially into the feature maps from the previous layer. The convolutional layer consists of 32 filters of size $3 \times 3 \times 3$ pixels. In convolutional layer, each feature map is constituted by several neurons having different values. These values are convoluted through the respective windows in the convolutional layer. The window size in the convolutional layer is usually 3×3 or 5×5. Here, the number of weight parameters changes accordingly. Finally, the outcomes are produced depending upon exciting activity at convolutional layer.

Pooling layer:

The operation in the convolutional layer is same as pooling layer. The difference of convolutional and pooling layer lies in the fact that the sliding window size is usually 2×2 in the lower sampling layer. Here, the sliding step is generally 2. This process halved the size of the feature map corresponding to the previous layer. Thus, the weight parameters for the CNN are reduced in a great extent. The pooling layer enables the classification model to become adaptive to the number of images. Also, it increases the overall speed of the classification model during training. The CRNN classification model uses an activation function called ReLU (Rectified Linear Unit).

RNN layer:

The important feature of recursive NN relays in the fact that it connects the hidden layers. Here, the nodes linked with each other from the input and hidden layers. In the proposed work, a unique type of recurrent NN called LSTM that is employed to learn the long-term dependence information. An LSTM is constituted by a memory cell with three multiplicative gates. The multiplicative gates consist of forget input and output. Information entering long short-term memory network can be judged by several rules. Here, the inconsistent data can be removed via the oblivion gate.

Merge layer:

The features extract via convolutional NN branch, also the features received from the recursive NN branch are merged utilizing merge layer. The merge layer uses a specified method to join the features from the convolutional NN and recursive NN. Here, an NN attention mechanism is used for selecting the specific features needed to classify the mammogram images. Here, an element-wise multiplication operation is used for merging the features.

Fully connected layer with softmax output:

The merged features from CNN and RNN layer have been fed to fully connected softmax layer. The output from softmax layer defines the probability distribution of all classes.

The proposed CRNN based mammogram images classification model is divided into two sections namely, CNN section and RNN branch. The CNN branch utilizes Xception mode with a transfer learning strategy for transferring the weight parameters to the RNN branch. The Xception consists of linear stack of separate convolutional layers connected in residual manner. The Xception model maps the individual output channel spatial correlation, then operates 1×1 depth convolution for obtaining cross-channel correlation. The deep separable convolutional layers in Xception reduce the complexity of the network. However, the RNN section or branch utilizes bi-directional long short term memory mode. At first, the pretrained parameters on the database are used by the weights in the CNN branch. Then, the RNN branch initializes the weight parameters randomly. During the training process, these weights are updated in an iterative manner. After a predetermined number of iterations, the training process is terminated.

The trained parameters are migrated to a new model with the help of transfer learning method. Here, the convolutional and the pooling layers of the pretrained Xception model are considered as the base of the classification model. The initialized weights from the task-specific fully connected layer have attached at the top of Xception model. Thus, the features are transmitted from the Xception model to the LSTM model.

The proposed CRNN model is trained in two phases. During the first phase, the entire convolution NN layers branch are frozen. At that time, final with recursive NN layer only trained. At the second phase, all the layers of the entire model are the learning rate of 0.0001. Finally, the loss functions in the model are optimized with the help of MOSOA. Here, the cross-entropy/accuracy is considered as the objective function in the CRNN based mammogram images classification model.

The neural network model incorporates the useful features from the CNN and the RNN branch to find the relevant features needed to obtain better classification results with improved accuracy. The proposed CRNN model automatically learns the critical features of the mammogram images. Thus, there is no need for manual feature extraction. Also, the use of transfer learning method for transferring the weight parameters to the convolutional NN branch enhances the robustness of CRNN framework.

The combined CRNN framework considers the spatial and temporal information present in the image, thereby learns the structural features of the images effectively. Then the merge layer output is specified to fully connected layer. At fully connected layer, the data is taken by nodes via the

output of merge layer, current input, final recurrent output. The fully connected layer and xth node is exhibited as

$$v_{Rx} = \widehat{\widehat{v}}_{Rx} + v_{(R-1)}d_{Rx} = q_x J_R^* + v_{(R-1)x}d_{Rx} = Q_x^j J_R^T + Q_x^f f_{R-1}^T + V_{(R-1)x}d_{Rx}, \tag{6}$$

where $q_x = \left(q_x^j, q_x^f\right) = \left(q_{x1}^j, q_{x2}^j, \ldots, q_{xl}^j, q_{x(k+1)}^{jf}, \ldots, q_{x(k+1)}^{*jf}\right)$ indicates weight vector then linked to pooling layer an xth fully connected layer node.

$$\widehat{\widehat{v}}_{Rx} = q_x J_x^*, x = 1, 2, \ldots, k, R = 1, 2, \ldots, r. \tag{7}$$

Here $i_{0x} = 0$, let $Q^* = \begin{bmatrix} q_1^* \\ \cdots \\ q_k^* \end{bmatrix}_{k\times(l+k)}$ as weight matrix that is linked to pooling layer including sum layer.

Numerous neurons are exists in CRNN, in which k count of nodes in RNN layer is expressed as:

$$K_{Rx}^{hidden} = \tan f\left(V_{Rx}\right) = \tan\left(\widehat{\widehat{V}}_{Rx} + V_{(R-1)}d_{Rx}\right). \tag{8}$$

when $d_{Rx} = 0, K_{Rx}^{hidden} = \tan f\left(V_{Rx}\right) Q_x^j J_R^T + Q_x^f f_{R-1}^T$. The tan$f$ function acts superior to log sig.

The delay deliberated the current RNN layer output vector feedback with its process is $f_R = (f_{R1}, f_{R2}, \ldots, f_{Rk})$. This process create the next pooling layer, the new pooling layer as $J_R^*(J_R, f_{R-1})^T$, the output layer specifies $v_R = (v_{R1}, v_{R2}, \ldots, v_{Rk})$, this input as well as outputs have employed to merge layer for attaining weight factor. The output node denotes z, then the output weight vector denotes $v_w = (v_{1w}, v_{2w}, \ldots, v_{kw})^T \in \aleph^k$ and this layer is linked to RNN layer along wth output node, and merging output on hidden layer including entire matrix as $c = (c_1, c_2, \ldots, c_z)_{kxz}$. The output layer activation function denotes $d(.)$. The output of RERNN classifier along wth specifies $(w = 1, 2, \ldots, z)$.

$$i_{Rw} = d\left(f_R c_w\right) = f_R c_w. \tag{9}$$

Here $R = 1, 2, \ldots, r, w = 1, 2, \ldots, z$ when the input imagery is trained the error process specifies R and Rth sample.

$$e_R\left(f_R c\right) = \frac{1}{2}\|u_R - i_R\|^2. \tag{10}$$

Here $u_R = (u_{R1}, u_{R2}, \ldots, u_{Rz})$, , and $i_R = f_R C = (j_{R1}, j_{R2}, \ldots, j_{Rz})$, R samples implicates error function.

$$e(y) = \sum_{R=1}^{r} e_R\left(f_R C\right). \tag{11}$$

Here $R = 1, 2, \ldots, r.$, $e_R\left(f_R C\right)$ signifies error function with Rth sample, $e(R+1)$ specifies error along $(R+1)$th samples, r specifies count of samples, the error functions including weight parameter specifies $R, j, x, \aleph$, by utilizing MOSOA, minimized the error functions.

3.2 | Optimized CRNN framework for classification of mammogram images

The optimized CRNN framework is well suited for classifying the mammogram images as it offers better exploration and exploitation ability with good convergence rate.

3.2.1 | Multi objective seagull optimization

In this work, multi objective seagull optimization (MOSOA) algorithm can be exploited to augment the convolutional recursive neural network (CRNN) for discovering the optimum parameters. Here multi objective seagull optimization algorithms are utilized for tuning the hyper parameters of CRNN. Usually, some methods are used for parameter configuration such as grid, manual, and random search model. Nevertheless, these search method are taking its peculiar weakness concerning iteration time and then, there is no stratagem-built knowledgeable exploration. Consequently, overwhelmed this weakness, multi objective seagull optimization algorithm is used. The MOSOA is deemed for tuning the hyper parameters of CRNN classifier to acquire the optimal parameters. Such parameters have been adjusted for acquiring great accuracy by lessening the errors along computational complexity. MOSOA[23] is inspired by the exploration and exploitation abilities of the seagulls. Seagull is a type of sea birds found

around the globe. There exist numerous varieties of seagulls along various lengths and weights. Seagulls are ubiquitous in nature; they consume small birds, fish, amphibians and so forth. An individual feature of the seagull is that it possesses a white plumage over the body. The seagulls' attacks fish with their feet and make a sound like rain for attracting the earthworms that found under the earth.

Movement for finding the best food source's location and frequent attacking for catching the prey are two main actions of seagulls.

Stepwise process of MOSOA

The stepwise process of MOSOA is explained as follows:

Step 1: Initialization.

The initial populations of the sea gull are initialized. From this, the populations of the sea gull is denoted as $a \leftarrow a + 1$.

Step 2: Random generation.

The input parameters are generated randomly after the initialization process. Here, the highest fitness values have chosen in terms of accurate hyper-parameter condition. To lessen the error rate, the population of procedure value is generated randomly.

Step 3: Fitness function.

This is estimated with optimum value to reach the objective function. The weight parameters of CRNN $(R, j, \aleph)$ are optimized by SOA. The parameters have developed with the help of population changes, the process of population changes has three stages for enhancing the CRNN parameters: delete (R), transform j, add $\aleph$.

Step 4: Position updation to diminish the computational complexity, error rate, and raising the accuracy.

The SOA describes the mating behavior of seagull including entire population.

Step 4.1: Exploration is utilized to lessen the error rate.

Population changes have estimated by lessening the error rate and changing colors depending on the season of subpopulation at each iteration. The change of population specifies ΨPop and subtracts all vector from the subpopulation indicates $iter_{pop}$, final data as $iter_{pop}^{y-1}$ its keep the changes of population vector.

$$iter_{pop} = iter_{pop} - iter_{pop}^{y-1}. \tag{12}$$

The color changing characteristics of seagull is depending on certain functions, namely, delete on (R), transform j, add $\aleph$.

Step 4.2: Exploitation is employed to lessen the computational complexity.

The overall count of population denotes $Seagull_{Pop}$, the count of seasons denotes z, the count of iteration signifies Max_{iter}, the count of subpopulation in every iteration signifies $Pop_{blue} \rightarrow blue$, $pop_{orange} \rightarrow orange$, $Pop_{yellow} \rightarrow yellow$. The computation complexity is minimized by maximizing the frequency iterations implies $\pi * 2$, overall population implicates $Pop_{Max} = \left(Seagull_{Pop} * 2/subpopul\right) - Pop_{Min}$, here subpopul = 3 along count of populations. The behavior of mating cyclic including polymorphic population along sine operations through the time with R vector begins with 0 along maximal count of iterations utilizing time space, frequency indicates $frequency * z$ including two auxiliary variables $A1 = \left[\frac{Pop_{\max}}{2}\right] + \left[\frac{Pop_{\min}}{2}\right]$ and $A2 = \left[\frac{Pop_{\max}}{2}\right] - \left[\frac{Pop_{\min}}{2}\right]$, where $A1$ and $A2$ specifies auxiliary variables. The subpopulation specifies each iteration $iter_{pop}$ for minimizing the computational complexity as:

$$iter_{pop} = A1 + A2 * \sin\left\{R + \left[\frac{frequecy}{popsub} * x\right]\right\}. \tag{13}$$

Let, x implies index values 1 to *popsub* along the overall seagull's populations.

Step 5: Termination.

The SOA is deemed to enhance the parameters of CRNN $(R, j, \aleph)$, also meets the objective functions by improving the accuracy as well as diminishing error rate with computational complexity. The better iterative positions together with fitness are determined, else repeat step 3 for obtaining more values.

Figure 3 depicts the flowchart of proposed MOSOA approach.

The pseudocode for the proposed MOSOA algorithm is given below (Algorithm 1):

Algorithm 1. MOSOA

Input: *Seagulls population.*

Initialize the parameters like the movement behaviors of search agents, A, the parameter that balances the exploration and exploitation phases, B and the maximum number of iterations or generations, Maxgen.

Find the fitness values for each search agents.

Find every non-dominated optimal Pareto solutions as well as initialize those optimal solutions for archiving space.

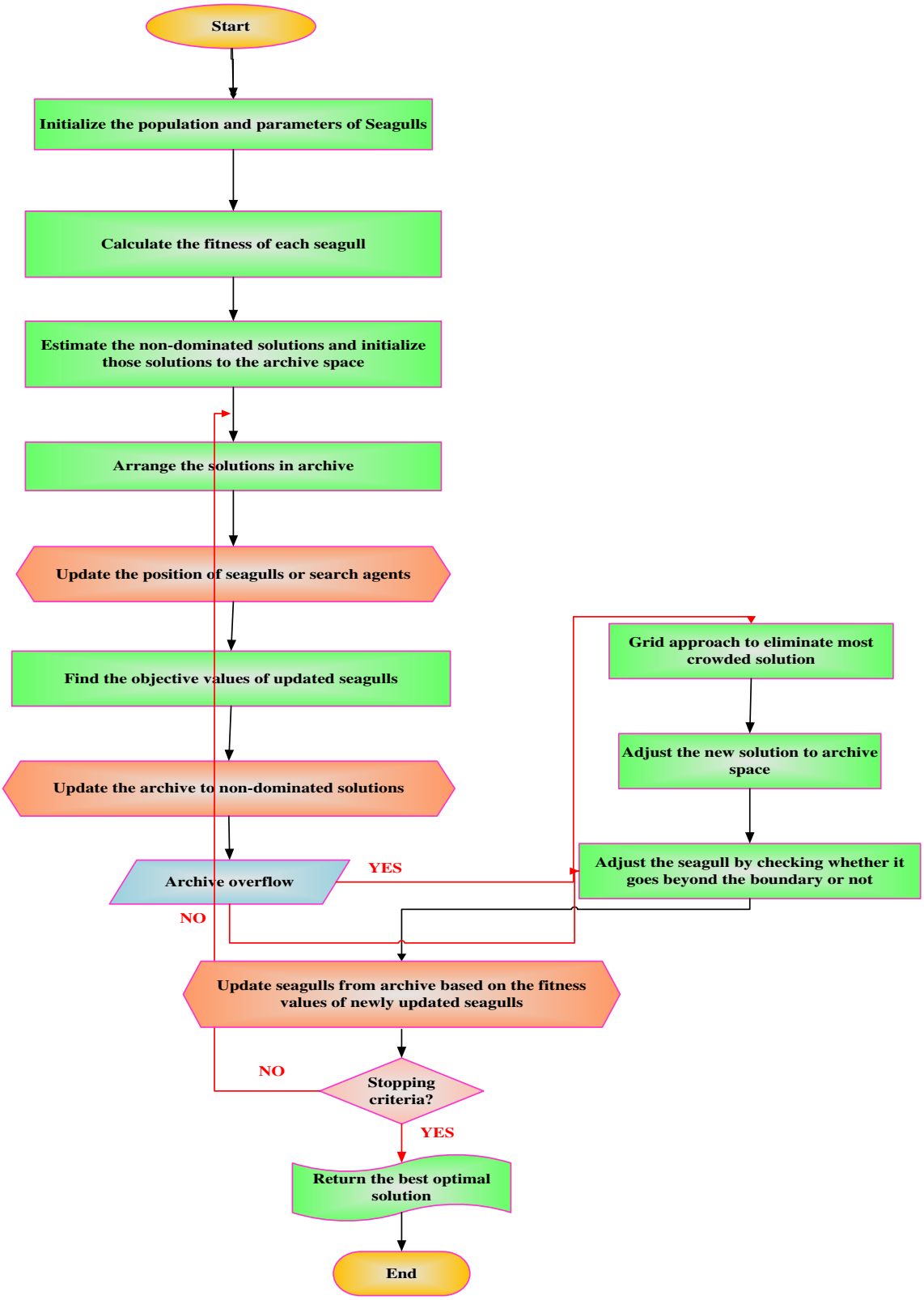

FIGURE 3 Flowchart of proposed multi-objective seagull optimization algorithm

while ($x < Maxgen$); *where, the parameter x represents the current iteration.*
for *each seagull.*
Update current seagull's position.
end for.
Estimate the fitness of all search agents.
From the updated search agents, find the non-dominated optimal Pareto solutions.
Update the acquired non-dominated optimal Pareto solutions for the space of archive.
if *the archive space is complete.*
Grid model is employed to eliminate a most crowded members in the archive space.
Add the new obtained solution for the space of archive.
end if.
Verify if any search agent moves beyond the search domain then adjust it.
Estimate every seagull fitness values.
$x \leftarrow x + 1$.
end while.
return the best optimal solution in the archive.
end
Output: *The non-dominated optimal solutions in the archive space.*

The proposed MOSOA possess multi-objectivity property with search space distinction. Also, an important advantage in MOSOA lies in the fact that it consists of archive search space for saving the POSs. Table 1 tabulates the parameter setting.

Computational complexity.

During fitness evaluation, the time complexity with maximal count of iterations, *Maxgen*, count of objectives, *f* and population size, *Popsize* is $O(Maxgen \times f \times popsize)$. The time taken to initialize the population is $O(popsize \times f)$. The proposed algorithm requires $O(L)$ time to select the leaders. The proposed MOSOA requires $O(f \times (s + popsize))$ time for updating the archive in non-dominated solutions, wherein the parameter *s* indicates ideal count of search agents or seagulls. Thus, the entire time complexity of the proposed algorithm denotes $O(Maxgen \times f \times (popsize + s) \times L)$ and space complexity during generation of population in memory requires $O(popsize \times f)$ time.

The fitness computation procedure and the updation of archive repeats until reach the maximal count of iterations.

The CRNN time complexity along *N* input images specifies $O\left(N^3\right)$. The overall time complexity of CRNN-MOSOA based classification process specifies $O\left(N^3 \times Maxgen \times f \times popsize\right)$, respectively.

In the proposed CRNN model, the training time taken by the Xception-LSTM during running over 80 epochs is approximately 15 h. Also, the testing time needed to test each mammogram image is approximately 3 s.

Thus, the optimized CRNN-MOSOA model provides better classification accuracy during mammogram images classification.

4 | EXPERIMENTAL RESULTS AND DISCUSSION

The proposed approach is done in MATLAB. From MAMMOSET dataset, the mammogram imageries are taken for evaluation.[24] The experimental results are compared with other existing methods, like deep learning computer-aided diagnosis for breast lesion in digital

TABLE 1 Parameter setting

Parameters	Numbers
Maxgen	200
Popsize	60
Count of runs	80
Grid inflation parameter, α	0.1
Leader selection parameter, β	4
Count of grids, G_{num}	10
ω_n (inertia weight)	[0, 1]

mammogram (BLIC-FrCN),[15] automatic detection and classification of mammograms using improved extreme learning machine with deep learning (BLIC-ICS-ELM)[16] and computer-aided diagnosis for variation among benign and malignant masses on breast DCE-MRI imageries utilizing deep convolutional neural network with Bayesian optimization (BLIC-DCNN-BO),[17] respectively.

4.1 | Dataset description

The MAMMOSET dataset consists of 11,183 mammogram imageries including 260 calcifications. Here, the mammogram imageries are classified as benign and malignant lesions. The minority class of calcification is deemed as outlier class, the non-calcification class is deemed as inliers. The size of every mammogram image represents 256×256 pixels.

4.2 | Performance evaluation

The classification performance of the proposed CRNN-MOSOA approach is evaluated utilizing certain performance metrices, namely, ROC curve, accuracy, F-measure, precision, recall, sensitivity, specificity, misclassified error (ME). Also, the performance is analyzed by several statistical measures, like skewness, kurtosis, mean, variance, and standard deviation (SD) to estimate the superiority of the CRNN-MOSOA classification framework.

The vital terms necessary to compute the performance metrics are expressed given below:

True positive (TP):

It reports abnormal into abnormal.

$$\mathrm{TP} = \frac{\mathrm{TP}}{\mathrm{TP} + \mathrm{FN}}. \tag{14}$$

True negative (TN):

It reports normal into normal.

$$\mathrm{TN} = \frac{\mathrm{TN}}{\mathrm{TN} + \mathrm{FP}}. \tag{15}$$

False positive (FP):

It reports abnormal into normal.

$$\mathrm{FP} = \frac{\mathrm{FP}}{\mathrm{FP} + \mathrm{TN}}. \tag{16}$$

False negative (FN):

It reports normal into abnormal.

$$\mathrm{FN} = \frac{\mathrm{FN}}{\mathrm{FN} + \mathrm{TP}}. \tag{17}$$

Sensitivity:

Sensitivity is computed by

$$\mathrm{Sensitivity} = \frac{\mathrm{TP}}{\mathrm{TP} + \mathrm{FN}}. \tag{18}$$

Specificity:

Specificity is computed by

$$\mathrm{Specificity} = \frac{\mathrm{TN}}{\mathrm{TN} + \mathrm{FP}}. \tag{19}$$

Precision:

It scales the positive predictive value.

$$\mathrm{Precision} = \frac{\mathrm{TP}}{\mathrm{TP} + \mathrm{FP}}. \tag{20}$$

Recall:

It scales the number of real positives that is properly predictable.

$$\text{Recall} = \frac{\text{TP}}{\text{TP} + \text{FN}}. \tag{21}$$

F-measure:

This is exhibited as

$$\text{F-measure} = 2\left(\frac{\text{Precision} * \text{Recall}}{\text{Precision} + \text{Recall}}\right). \tag{22}$$

Accuracy:

This is the classification capability suitable for the entire number of classification tests.

$$\text{Accuracy} = \frac{\text{TP} + \text{TN}}{\text{TP} + \text{FN} + \text{FP} + \text{TN}}. \tag{23}$$

ROC (receiver operating characteristics) curve.:

This is a graph showing classification mode presentation in every classification thresholds. This curve plots two parameters called the true positive rate (TPR) and false positive rate (FPR).

Misclassified error rate:

During classification, the misclassified error (ME) is estimated using the following expression

$$\text{ME} = \frac{\text{FP} + \text{FN}}{\text{TP} + \text{FN} + \text{FP} + \text{TN}}. \tag{24}$$

Mean:

Mean refers to the average value of the intensity of the image. It is calculated using the given equation

$$\text{Mean}, \eta = \sum_{i=1}^{m} ip(i). \tag{25}$$

In the above expression, the parameter p represents the independent data vectors.

Variance:

Variance depicts the intensity variation around the mean. It is calculated with the following equation

$$\text{Variance}, \sigma^2 = \sum_{i=1}^{m} (i - \eta)^2 p(i). \tag{26}$$

Standard deviation:

In SD, σ refers to the estimation of mean square deviation of the pixel value $p(i, j)$ from its mean value. It is determined using the given formula:

$$\sigma = \sqrt{\text{Variance}} = \left(\sum_{i=1}^{m} (i - \eta)^2 p(i)\right)^{1/2}. \tag{27}$$

Skewness:

Skewness measure depicts the symmetries of the histogram around the mean. It is calculated as

$$\text{Skewness} = \frac{\sum_i^m \left(y_i - \overline{y}\right)^3}{(m-1) * \sigma^2} \tag{28}$$

Kurtosis:

Kurtosis depicts the flatness of the histogram. It is derived using the given equation

$$\text{Kurtosis} = \frac{\eta^4}{\sigma^4} \tag{29}$$

4.3 | Results

The classified categories representation of mammogram images by using the proposed CRNN-MOSOA based classification model, which is depicted in Figure 4.

Figures 5–13 shows the simulation result of accuracy, sensitivity, specificity, precision, recall, F-score, ROC curve, skewness, kurtosis, mean, variance, SD, and ME obtained from the proposed BLIC-CRNN-MOSOA is likened to the existing BLIC-FrCN, BLIC-ICS-ELM, and BLIC-DCNN-BO methods, respectively.

4.4 | Discussion

Figure 5 shows the comparison of accuracy of the proposed BLIC-CRNN-MOSOA approach with other existing methods like BLIC-FrCN, BLIC-ICS-ELM, and BLIC-DCNN-BO, respectively. For training–testing (50%–50%), the accuracy of proposed BLIC-CRNN-MOSOA method provides 4.56%, 2.45%, and 11.31% better accuracy likened to the existing BLIC-FrCN, BLIC-ICS-ELM and BLIC-DCNN-BO, respectively. For training–testing (60%–40%), the accuracy of proposed BLIC-CRNN-MOSOA method provides 25.74%, 16.08%. and 21.15% better accuracy likened to the existing BLIC-FrCN, BLIC-ICS-ELM, and BLIC-DCNN-BO, respectively. For training–testing (70%–30%), the accuracy of proposed BLIC-CRNN-MOSOA method provides 7.60%, 5.78%, and 32.29% better accuracy likened to the existing BLIC-FrCN, BLIC-ICS-ELM, and BLIC-DCNN-BO, respectively. For training–testing (80%–20%), the accuracy of proposed BLIC-CRNN-MOSOA method provides 15.23%, 22.56%, and 16.03% better accuracy likened to the existing BLIC-FrCN, BLIC-ICS-ELM, and BLIC-DCNN-BO, respectively. For training–testing (90%–10%), the accuracy of proposed BLIC-CRNN-MOSOA method provides 23.11%, 42.03%, and 52.23% better accuracy likened to the existing BLIC-FrCN, BLIC-ICS-ELM, and BLIC-DCNN-BO, respectively.

Figure 6 shows the comparison of sensitivity of the proposed BLIC-CRNN-MOSOA approach with other existing methods like BLIC-FrCN, BLIC-ICS-ELM, and BLIC-DCNN-BO, respectively. For training–testing (50%–50%), the sensitivity of proposed BLIC-CRNN-MOSOA method provides 34.67%, 13.10%, and 51.06% better sensitivity likened to the existing BLIC-FrCN, BLIC-ICS-ELM, and BLIC-DCNN-BO, respectively. For training–testing (60%–40%), the sensitivity of proposed BLIC-CRNN-MOSOA method provides 15.33%, 22.56%, and 39.22% better sensitivity likened to the existing BLIC-FrCN, BLIC-ICS-ELM, and BLIC-DCNN-BO, respectively. For training–testing (70%–30%), the sensitivity of

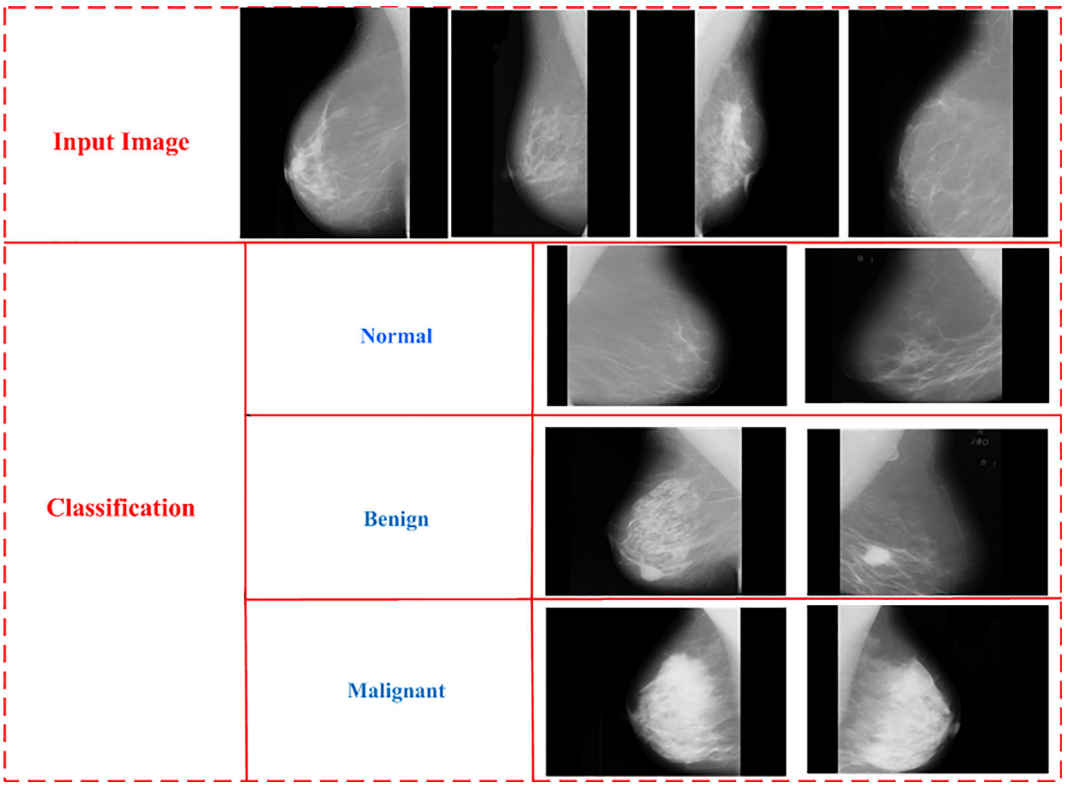

FIGURE 4 Classified categories representation of mammogram images utilizing proposed CRNN-MOSOA model

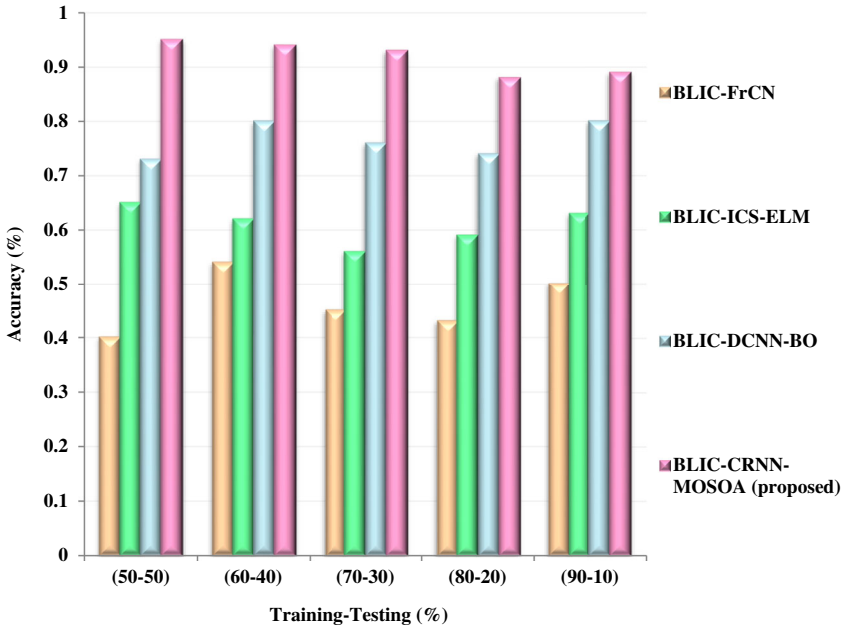

FIGURE 5 Performance comparison of accuracy

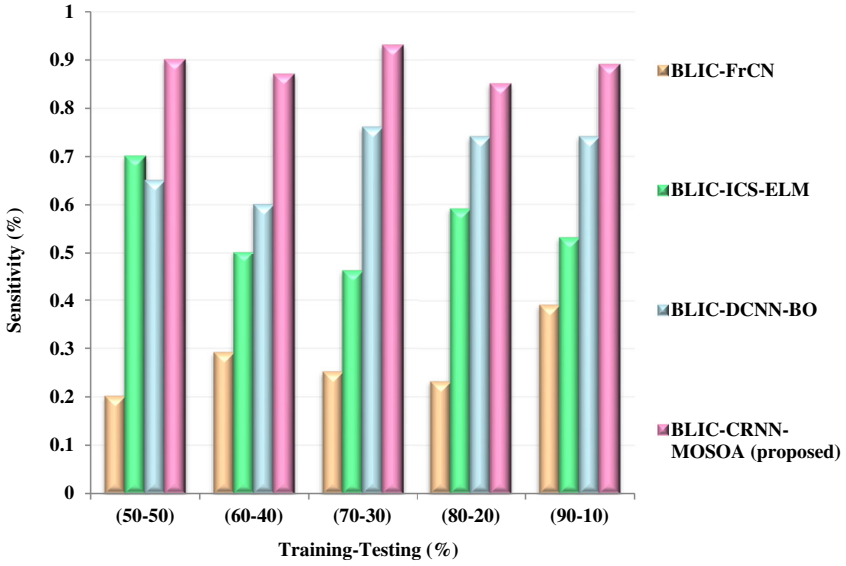

FIGURE 6 Performance comparison of sensitivity

proposed BLIC-CRNN-MOSOA method provides 7.60%, 5.78%, and 32.29% better sensitivity likened to the existing BLIC-FrCN, BLIC-ICS-ELM, and BLIC-DCNN-BO, respectively. For training–testing (80%–20%), the sensitivity of proposed BLIC-CRNN-MOSOA method provides 41.29%, 24.25%, and 31.33% better sensitivity likened to the existing BLIC-FrCN, BLIC-ICS-ELM, and BLIC-DCNN-BO, respectively. For training–testing (90%–10%), the sensitivity of proposed BLIC-CRNN-MOSOA method provides 11.23%, 30.21%, and 25.36% better sensitivity likened to the existing BLIC-FrCN, BLIC-ICS-ELM, and BLIC-DCNN-BO.

Figure 7 displays the comparison of specificity of BLIC-CRNN-MOSOA approach with other existing methods like BLIC-FrCN, BLIC-ICS-ELM, and BLIC-DCNN-BO, respectively. For training–testing (50%–50%), the specificity of proposed BLIC-CRNN-MOSOA method provides 33.49%, 26.97%, and 21.06% better specificity likened to the existing BLIC-FrCN, BLIC-ICS-ELM, and BLIC-DCNN-BO, respectively. For training–testing (60%–40%), the specificity of proposed BLIC-CRNN-MOSOA method provides 5.23%, 2.55%, and 20.15% better specificity likened to the existing BLIC-FrCN, BLIC-ICS-ELM, and BLIC-DCNN-BO, respectively. For training–testing (70%–30%), the specificity of proposed BLIC-CRNN-MOSOA method provides 23.45%, 36.22%, 29.29% better specificity likened to the existing BLIC-FrCN, BLIC-ICS-ELM, and BLIC-DCNN-BO, respectively.

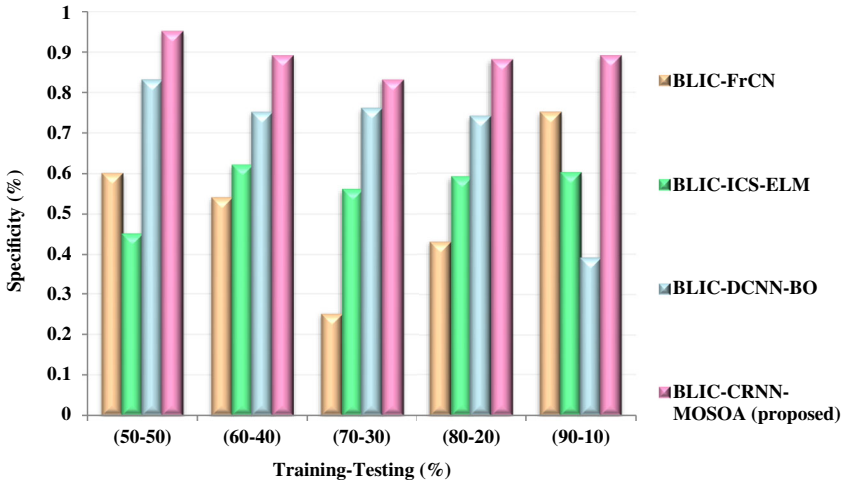

FIGURE 7 Performance comparison of specificity

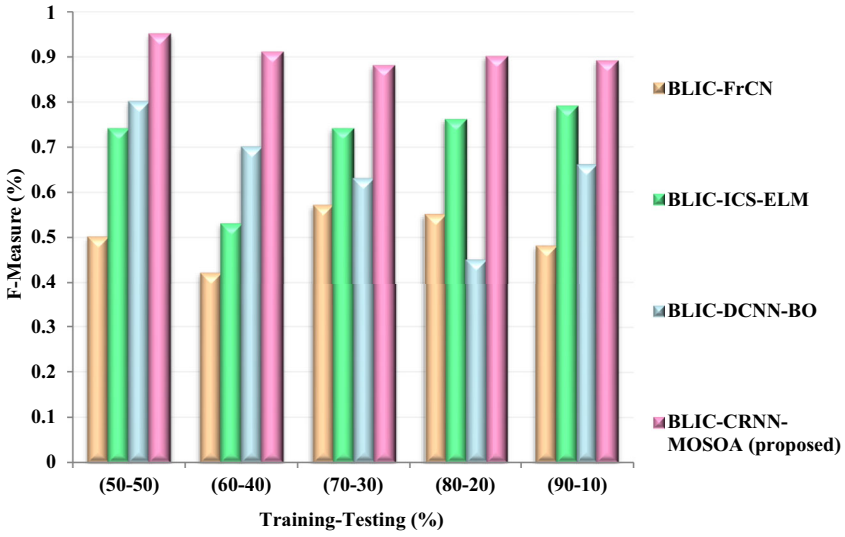

FIGURE 8 Performance comparison of F-measure

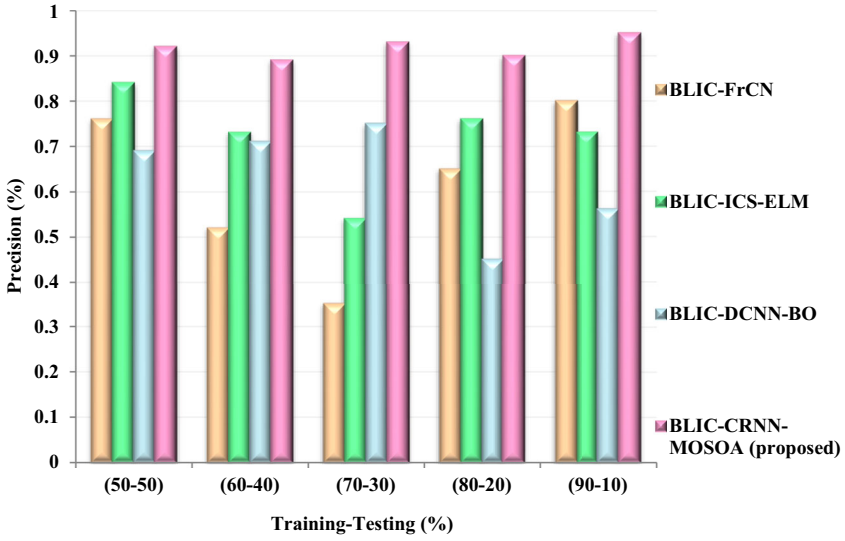

FIGURE 9 Performance comparison of precision

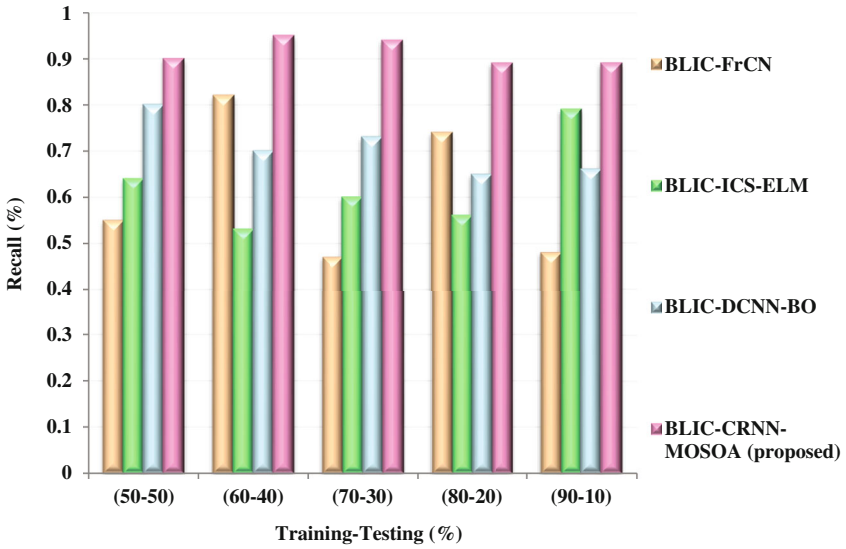

FIGURE 10 Performance comparison of recall

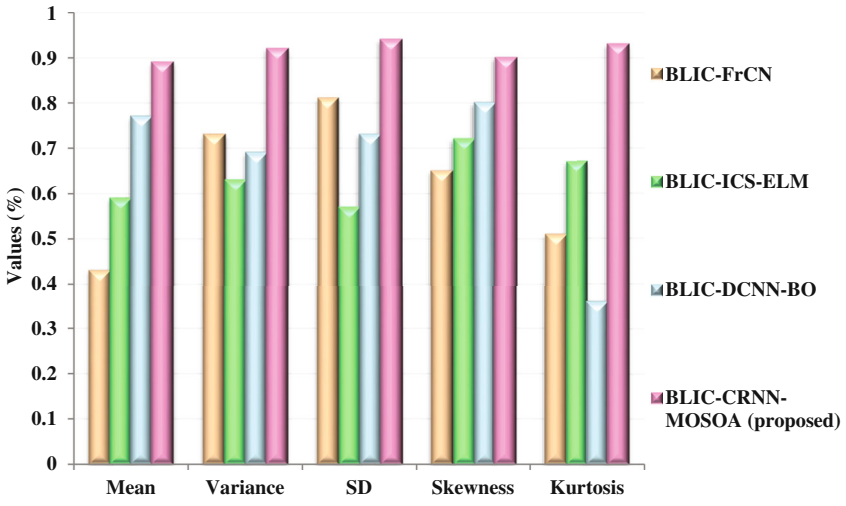

FIGURE 11 Performance comparison of mean, variance, SD, skewness, and kurtosis

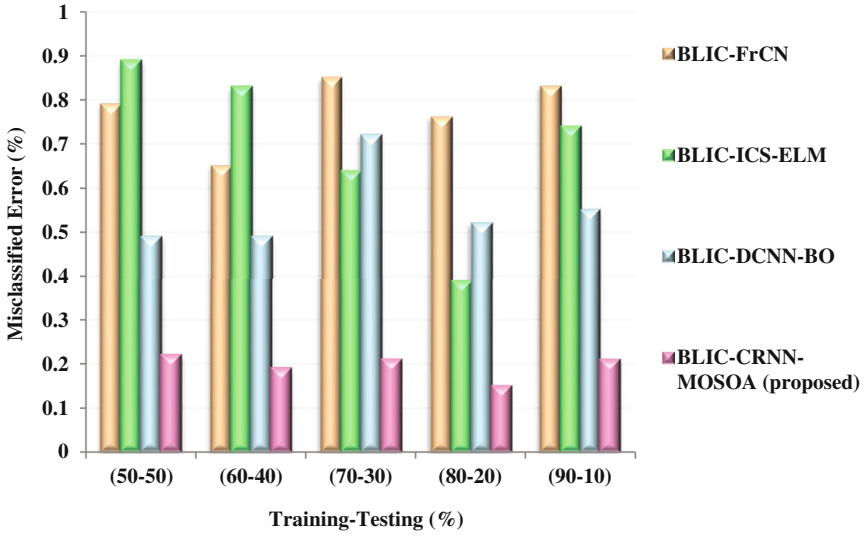

FIGURE 12 Performance comparison of misclassified error

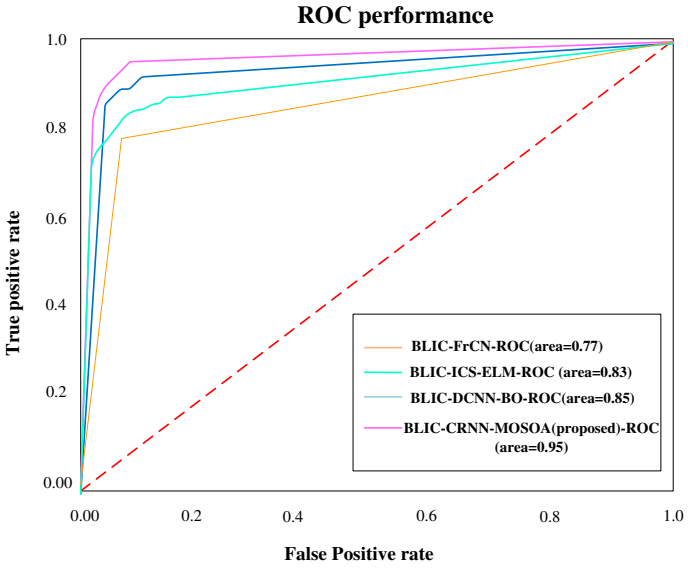

FIGURE 13 Performance comparison of AUC

For training–testing (80%–20%), the specificity of proposed BLIC-CRNN-MOSOA method provides 24.7%, 33.5%, and 61.03%better specificity likened to the existing BLIC-FrCN, BLIC-ICS-ELM, and BLIC-DCNN-BO, respectively. For training–testing (90%–10%), the specificity of proposed BLIC-CRNN-MOSOA method provides 9.33%, 28.12%, and 33.24% better specificity likened to the existing BLIC-FrCN, BLIC-ICS-ELM, and BLIC-DCNN-BO, respectively.

Figure 8 shows the comparison of F-measure of the proposed BLIC-CRNN-MOSOA approach with other existing methods like BLIC-FrCN, BLIC-ICS-ELM, and BLIC-DCNN-BO, respectively. For training–testing (50%–50%), the F-measure of proposed BLIC-CRNN-MOSOA method provides 21.45%, 30.38%, and 21.01% better F-measure likened to existing BLIC-FrCN, BLIC-ICS-ELM, and BLIC-DCNN-BO, respectively. For training–testing (60%–40%), the F-measure of proposed BLIC-CRNN-MOSOA method provides 20.56%, 31.34%, and 25.13% better F-measure likened to existing BLIC-FrCN, BLIC-ICS-ELM, and BLIC-DCNN-BO, respectively. For training–testing (70%–30%), the F-measure of proposed BLIC-CRNN-MOSOA method provides 25.53%, 36.27%, and 23.09% better F-measure likened to existing BLIC-FrCN, BLIC-ICS-ELM, and BLIC-DCNN-BO, respectively. For training–testing (80%–20%), the F-measure of proposed BLIC-CRNN-MOSOA method provides 36.44%, 21.11%, and 31.55% better F-measure likened to existing BLIC-FrCN, BLIC-ICS-ELM, and BLIC-DCNN-BO, respectively. For training–testing (90%–10%), the F-measure of proposed BLIC-CRNN-MOSOA method provides 13.32%, 18.03%, and 22.36% better F-measure likened to existing BLIC-FrCN, BLIC-ICS-ELM, and BLIC-DCNN-BO.

Figure 9 displays the comparison of precision of BLIC-CRNN-MOSOA approach with other existing methods like BLIC-FrCN, BLIC-ICS-ELM, and BLIC-DCNN-BO, respectively. For training–testing (50%–50%), the precision of proposed BLIC-CRNN-MOSOA method provides 10.22%, 51.36%, and 15.26% better precision likened to existing BLIC-FrCN, BLIC-ICS-ELM, and BLIC-DCNN-BO, respectively. For training–testing (60%–40%), the precision of proposed BLIC-CRNN-MOSOA method provides 30.52%, 15.22%, and 11.66% better precision likened to existing BLIC-FrCN, BLIC-ICS-ELM, and BLIC-DCNN-BO, respectively. For training–testing (70%–30%), the precision of proposed BLIC-CRNN-MOSOA method provides 22.31%, 11.25%, and 30.52% better precision likened to existing BLIC-FrCN, BLIC-ICS-ELM, and BLIC-DCNN-BO, respectively. For training–testing (80%–20%), the precision of proposed BLIC-CRNN-MOSOA method provides 13.52%, 10.03%, and 19.05% better precision likened to existing BLIC-FrCN, BLIC-ICS-ELM, and BLIC-DCNN-BO, respectively. For training–testing (90%–10%), the precision of proposed BLIC-CRNN-MOSOA method provides 16.15%, 23.15%, and 55.13% better precision likened to existing BLIC-FrCN, BLIC-ICS-ELM, and BLIC-DCNN-BO, respectively.

Figure 10 portrays the comparison of recall of the proposed BLIC-CRNN-MOSOA approach with other existing methods like BLIC-FrCN, BLIC-ICS-ELM, and BLIC-DCNN-BO, respectively. For training–testing (50%–50%), the recall of proposed BLIC-CRNN-MOSOA method provides 20.36%, 26.27%, and 11.06% better recall likened to existing BLIC-FrCN, BLIC-ICS-ELM, and BLIC-DCNN-BO, respectively. For training–testing (60%–40%), the recall of proposed BLIC-CRNN-MOSOA method provides 20.43%, 26.19%, and 13.06% better recall likened to existing BLIC-FrCN, BLIC-ICS-ELM, and BLIC-DCNN-BO, respectively. For training–testing (70%–30%), the recall of proposed BLIC-CRNN-MOSOA method provides 13.29%, 10.19%, and 33.16% higher recall compared with the existing methods like BLIC-FrCN, BLIC-ICS-ELM, and BLIC-DCNN-BO, respectively. For training–testing (80%–20%), the recall of proposed BLIC-CRNN-MOSOA method provides 20.52%, 17.03%, and 15.55% higher recall compared with the existing methods like BLIC-FrCN, BLIC-ICS-ELM, and BLIC-DCNN-BO, respectively. For training–testing (90%–10%), the recall

of proposed BLIC-CRNN-MOSOA method provides 11.15%, 9.15%, and 23.26% better recall likened to existing BLIC-FrCN, BLIC-ICS-ELM, and BLIC-DCNN-BO, respectively.

Figure 11 shows the comparison of mean, variance, SD, skewness and kurtosis of the proposed BLIC-CRNN-MOSOA approach with other existing methods like BLIC-FrCN, BLIC-ICS-ELM, and BLIC-DCNN-BO, respectively. The mean of the proposed BLIC-CRNN-MOSOA method provides 34.63%, 26.75%, and 31.24% higher mean compared with the existing methods like BLIC-FrCN, BLIC-ICS-ELM, and BLIC-DCNN-BO, respectively. The variance of proposed BLIC-CRNN-MOSOA method provides 45.67%, 34.53%, and 63.01% higher variance compared with the existing methods like BLIC-FrCN, BLIC-ICS-ELM, and BLIC-DCNN-BO, respectively. The SD of proposed BLIC-CRNN-MOSOA method provides 34.95%, 26.67%, and 13.33% better SD likened to existing BLIC-FrCN, BLIC-ICS-ELM, and BLIC-DCNN-BO, respectively. The skewness of proposed BLIC-CRNN-MOSOA method provides 25.36%, 42.31%, and 33.42% higher skewness compared with the existing methods like BLIC-FrCN, BLIC-ICS-ELM, and BLIC-DCNN-BO, respectively. The kurtosis of proposed BLIC-CRNN-MOSOA method provides 13.21%, 11.31%, and 25.05% higher kurtosis compared with the existing methods like BLIC-FrCN, BLIC-ICS-ELM, and BLIC-DCNN-BO, respectively.

Figure 12 shows the comparison of misclassified error of the proposed BLIC-CRNN-MOSOA approach with other existing methods like BLIC-FrCN, BLIC-ICS-ELM, and BLIC-DCNN-BO, respectively. For training–testing (50%–50%), the misclassified error of proposed BLIC-CRNN-MOSOA attains 33.36%, 11.63%, 30.59% lower misclassified error likened to existing BLIC-FrCN, BLIC-ICS-ELM, and BLIC-DCNN-BO, respectively. For training–testing (60%–40%), the misclassified error of proposed BLIC-CRNN-MOSOA method provides 24.12%, 57.28%, and 43.13% lower misclassified error compared with the existing methods like BLIC-FrCN, BLIC-ICS-ELM, and BLIC-DCNN-BO, respectively. For training–testing (70%–30%), the misclassified error of proposed BLIC-CRNN-MOSOA method provides 69.4%, 67.33%, and 35.55% lower misclassified error compared with the existing methods like BLIC-FrCN, BLIC-ICS-ELM, and BLIC-DCNN-BO, respectively. For training–testing (80%–20%), the misclassified error of proposed BLIC-CRNN-MOSOA method provides 22.6%, 34.67%, and 45.7% lower misclassified error compared with the existing methods like BLIC-FrCN, BLIC-ICS-ELM, and BLIC-DCNN-BO, respectively. For training–testing (90%–10%), the misclassified error of proposed BLIC-CRNN-MOSOA method provides 11.08%, 30.41%, and 21.32% lower misclassified error compared with the existing methods like BLIC-FrCN, BLIC-ICS-ELM, and BLIC-DCNN-BO, respectively. Figure 13 figure shows the performance comparison of AUC.

The enhancement of area under curve is scaled using DeLong approach. The area under curve should measure for variables that are statistically significant outcome, hence argue against testing the null hypothesis of indifference for nested area under curves. The rise in area under curves is expressed as a confidence interval that is generated with the help of DeLong-based strategy once the statistical significance of the extra variable is assessed.

Here D denotes interest outcome with $D = 1$ for disease and $D = 0$ for non-disease. Prediction of event status utilizing P test results are denoted in Equation (30),

$$X = X_1, \ldots, X_P. \tag{30}$$

From Equation (30), D and X vector are obtainable for N patients. The disease prediction depending on entire set of P test results is analyzed with decreased count of tests is denoted as $P-1$. A disease-prediction model is deemed to scale the risk score with logistic regression or LDA. It creates linear coefficients and it assesses for entire model and the decreased model is expressed in Equations (31) and (32) as follows:

$$a' = [a_1, \ldots, a_P], \tag{31}$$

$$a'_R = \left(a_1^R, \ldots, a_{p-k}^R\right). \tag{32}$$

To check whether the disease prediction model with P predictors discriminates among the two subgroups greater than the model is calculated using AUC as a measure of model performance and formulated using hypothesis as expressed in Equation (33) as follows:

$$\begin{aligned} H_0^{AUC} &: AUC_P = AUC_{P-k}, \\ H_a^{AUC} &: AUC_P \neq AUC_{P-k}. \end{aligned} \tag{33}$$

Here AUC_P, AUC_{P-k} represents area under curves of full and reduced model. The parametric AUC estimator available in multivariate normal case is denoted as $eAUC$ in which e stands for empirical and is given in Equation (34) as follows:

$$eAUC = \frac{1}{n_0 n_1} \sum_{x_i \in D_0} \sum_{x_j \in D_1} I\left[a' x_i, a' x_j\right]. \tag{34}$$

Here D_1 and D_2 represents classification of disease with and without Breast Lesion, respectively, n_1 and n_0 denotes the grade of disease and $I\left[a' x_i, a' x_j\right]$ represents the indicator function. DeLong approach is better estimating linear coefficients and the formula of AUC is represented in Equation (35)

$$AUC = \Phi\left(\sqrt{\frac{(\mu_1 - \mu_0)\sum^{-1}(\mu_1 - \mu_0)}{2}}\right), \tag{35}$$

where $\Phi\left(\sqrt{\frac{(\mu_1-\mu_0)\sum^{-1}(\mu_1-\mu_0)}{2}}\right)$ denotes the standard normal cumulative distributive function. The proposed BLIC-CRNN-MOSOA model has outperformed existing methods by offering a highest AUC value. For instance, the existing BLIC-FrCN model has attained a lower AUC value of 0.77, whereas slightly higher AUC value of 0.83 and 0.85 has been offered by existing BLIC-ICS-ELM and BLIC-DCNN-BO, respectively. But, the proposed BLIC-CRNN-MOSOA model has exhibited superior outcome with the maximum AUC value is 98. The proposed BLIC-CRNN-MOSOA model provides 43.19%, 69.59%, and 52.43% greater AUC than the existing methods, like BLIC-FrCN, BLIC-ICS-ELM, and BLIC-DCNN-BO, respectively.

4.5 | Justification of result

By utilizing a single modality, the classification task for differentiating cancer from other abnormalities in a lesion-based analysis, the areas under the ROC curves are significantly raised when the system selected the mode (mean, minimum, maximum), here image-based features are joint in lesion-based features. The performance is determined for lesion-based analysis and automated feature selection from both modalities. The proposed model classified the mammogram images that helps early diagnosis of breast cancer. Simulation results prove that the proposed BLIC-CRNN-MOSOA method attains better results compared to the BLIC-FrCN, BLIC-ICS-ELM, and BLIC-DCNN-BO, respectively. The proposed BLIC-CRNN-MOSOA provide higher accuracy 98.58%, 95.36%, and 93.87%, higher sensitivity 93.64%, 90.23%, and 91.91%, higher specificity 92.67%, 91.28%, and 95.39%, higher F-measure 89.31%, 90.78%, and 96.34% higher precision 95.56%, 92.37%, and 93.31% higher recall 87.69%, 93.57, and 88.47% and lower misclassified error 92.41%, 95.39%, and 96.69% compared with existing method BLIC-FrCN, BLIC-ICS-ELM, and BLIC-DCNN-BO, respectively.

5 | CONCLUSION

An efficient breast cancer image classification combines the advantages of CNN and RNN for the categorization of breast lesions as normal, benign, and malignant is proposed in this article. Here, a global optimizer namely, the multi-objective seagull optimization approach is considered to optimize the weight parameters for CRNN framework. At first, the unnecessary noise components from the raw mammogram imageries are removed for better boundary detection using an APPDRC approach. Then, the most relevant features essential for classification of breast cancer images are extracted. Finally, an optimized CRNN model is utilized for classifying the mammogram images. The proposed approach is done in MATLAB, its efficiency is analyzed with existing approaches. When compared to the existing methods, the proposed method attains better improved accuracy of about 99.4%, sensitivity of about 97.8%, specificity of about 98.2%, precision of about 97.6%, recall of about 96.7%, and f-measure of about 97%.This breast lesion identification and categorization using mammography screening technique is appropriate on the real time applications. This technique is also able to classify the breast lesions status by collecting real time data at various health care services. Besides, this technique efficiently categorizes the breast lesion. Also, this technique compares the accuracy of various deep learning strategies that is employed for identifying the breast lesion in beginning stage. When estimated with other deep learning classifier models, the proposed model offers better prediction with classification tasks. These tasks can be employed for disease probability prediction, diagnosis, screening, treatment guidance and complication management. This application implicates a promising tool to help the breast lesions. The utilization of high-performance computing (HPC) applications can pave the way for enhanced healthcare and the effectual lessening and control of breast lesion. In future, these high-performance computing strategies will effectually control the disease. HPC is helpful for processing large-scale data of individuals and it is helpful for storing intermediate results or processing large-scale data.

CONFLICT OF INTEREST

The authors state that they have no competing financial interests or personal relationships that could have an impact on the work reported here.

DATA AVAILABILITY STATEMENT

Data sharing does not apply to this article as no new data were created or examined here.

ORCID

N. K. Sakthivel https://orcid.org/0000-0003-1772-9204

REFERENCES

1. Zheng S, Jayasumana S, Romera-Paredes B et al. Conditional random fields as recurrent neural networks. Proceedings of the IEEE International Conference on Computer Vision; 2015:1529-1537.
2. Lapa P, Castelli M, Gonçalves I, Sala E, Rundo L. A hybrid end-to-end approach integrating conditional random fields into CNNs for prostate cancer detection on MRI. *Appl Sci*. 2020;10(1):338.
3. Rundo L, Militello C, Vitabile S, Russo G, Sala E, Gilardi MC. A survey on nature-inspired medical image analysis: a step further in biomedical data integration. *Fundam Inform*. 2020;171(1–4):345-365.
4. Osaba E, Yang XS. Applied optimization and swarm intelligence: a systematic review and prospect opportunities. In: Osaba E, Yang XS, eds. *Applied Optimization and Swarm Dermatol Int*. Springer; 2021:1-23.
5. Yang Z, Cao Z, Zhang Y, et al. MommiNet-v2: mammographic multi-view mass identification networks. *Med Image Anal*. 2021;73:102204.
6. Bria A, Marrocco C, Tortorella F. Addressing class imbalance in deep learning for small lesion detection on medical images. *Comput Biol Med*. 2020;120:103735.
7. Castiglioni I, Rundo L, Codari M, et al. AI applications to medical images: from machine learning to deep learning. *Phys Med*. 2021;83:9-24.
8. Militello C, Vitabile S, Rundo L, Russo G, Midiri M, Gilardi MC. A fully automatic 2D segmentation method for uterine fibroid in MRgFUS treatment evaluation. *Comput Biol Med*. 2015;62:277-292.
9. Kumar SN, Fred AL, Varghese PS. Suspicious lesion segmentation on brain, mammograms and breast MR images using new optimized spatial feature based super-pixel fuzzy c-means clustering. *J Digit Imaging*. 2019;32(2):322-335.
10. Shajin FH, Rajesh P. Trusted secure geographic routing protocol: outsider attack detection in mobile ad hoc networks by adopting trusted secure geographic routing protocol. *Int J Pervasive Comput Commun*. 2020. doi:10.1108/IJPCC-09-2020-0136
11. Thota MK, Shajin FH, Rajesh P. Survey on software defect prediction techniques. *Int J Appl Sci Eng*. 2020;17(4):331-344.
12. Siegel RL, Miller KD, Fedewa SA, et al. Colorectal cancer statistics, 2017. *CA Cancer J Clin*. 2017;67(3):177-193.
13. Subasree S, Gopalan NP, Sakthivel NK. EMOPS: an enhanced multi-objective Pswarm based classifier for poorly understood cancer patterns. *Int J Eng Technol*. 2018;7(2.27):7-11.
14. Harford JB. Breast-cancer early detection in low-income and middle-income countries: do what you can versus one size fits all. *Lancet Oncol*. 2011;12(3):306-312.
15. Al-Antari MA, Al-Masni MA, Kim TS. Deep learning computer-aided diagnosis for breast lesion in digital mammogram. *Adv Exp Med Image Biol*. 2020;1213:59-72.
16. Chakravarthy SS, Rajaguru H. Automatic detection and classification of mammograms using improved extreme learning machine with deep learning. *IRBM*. 2021;43:49-61.
17. Hizukuri A, Nakayama R, Nara M, Suzuki M, Namba K. Computer-aided diagnosis scheme for distinguishing between benign and malignant masses on breast DCE-MRI images using deep convolutional neural network with Bayesian optimization. *J Digit Imaging*. 2021;34(1):116-123.
18. Al-Antari MA, Han SM, Kim TS. Evaluation of deep learning detection and classification towards computer-aided diagnosis of breast lesions in digital X-ray mammograms. *Comput Methods Programs Biomed*. 2020;196:105584.
19. Melekoodappattu JG, Subbian PS. Automated breast cancer detection using hybrid extreme learning machine classifier. *J Ambient Intell Humaniz Comput Secur*. 2020. 1(1)1-10.
20. Cao Z, Duan L, Yang G, Yue T, Chen Q. An experimental study on breast lesion detection and classification from ultrasound images using deep learning architectures. *BMC Med Imaging*. 2019;19(1):1-9.
21. Sadr H, Pedram MM, Teshnehlab M. A robust sentiment analysis method based on sequential combination of convolutional and recursive neural networks. *Neural Process Lett*. 2019;50(3):2745-2761.
22. Liang G, Hong H, Xie W, Zheng L. Combining convolutional neural network with recursive neural network for blood cell image classification. *IEEE Access*. 2018;3:36188-36197.
23. Dhiman G, Singh KK, Soni M, et al. MOSOA: a new multi-objective seagull optimization algorithm. *Expert Syste Appl*. 2021;167:114150.
24. Oliveira PH, Scabora LC, Cazzolato MT, Bedo MV, Traina AJ, Traina Jr C. MAMMOSET: an enhanced dataset of mammograms. Proceedings of the Satellite Events of the Brazilian Symposium on Databases; 2017:256-266; SBC.

How to cite this article: Sakthivel NK, Subasree S, Alias Priya M P, Tyagi AK. Breast lesion identification and categorization using mammography screening based on combined convolutional recursive neural network framework with parameters optimized using multi-objective seagull optimization algorithm. *Concurrency Computat Pract Exper*. 2022;e7348. doi: 10.1002/cpe.7348